Pb dominant members of crandallite group from Cínovec and Moldava deposits, Krušné hory Mts. (Czech Republic)

Pb dominantní členy skupiny crandallitu z ložisek Cínovec a Moldava, Krušné hory (Česká republika) (Czech summary)

(15 text-figs)

JIŘÍ SEJKORA [1] – JIŘÍ ČEJKA [2] – VLADIMÍR ŠREIN [3]

[1] *Department of Mineralogy and Petrology, National Museum Prague, Václavské nám. 68, CZ-115 79 Praha 1, Czech Republic, jiri.sejkora@nm.cz*
[2] *Natural History Museum, National Museum Prague, Václavské nám. 68, CZ-115 79, Praha 1, Czech Republic, jiri.cejka@nm.cz*
[3] *Institute of Rock Structure and Mechanics, Academy of Science of Czech Republic, V Holešovičkách 41, CZ-182 09 Praha 8, Czech Republic, srein@alpha.irms.cas.cz*

Pb dominant members of crandallite group from Cínovec Sn-W deposit and Moldava fluorite deposit (Krušné hory Mts., Czech Republic) were studied by X-ray powder diffraction, chemical analyses and infrared spectroscopy. The minority content of indium (up to 2.44 wt. % In_2O_3) in the B position of general formula observed in beudantite sample from Cínovec is the first known assertion of this chemical element in minerals of the crandallite group.
The pronounced dependence of the lattice parameters on the Al/Fe ration in B position and As/P in X position of general formula for Pb-dominant members of crandallite group was established. Extensive isomorphism in all three positions in general formula of the crandallite group minerals was confirmed.

Key words: crandallite group, philipsbornite, plumbogummite, segnitite, beudantite, indium, chemical analysis, X-ray powder diffraction, infrared spectroscopy, Cínovec, Moldava, Czech Republic

Introduction

Composition of mineral phases included in the crandallite group, also called the alunite – jarosite family, can be characterized by the general formula $AB_3(XO_4)_2(OH)_6$ or $AB_3(XO_4)(XO_3OH)(OH)_6$. However, some authors (e. g. Mandarino 1999) separate this extensive group in alunite, beudantite and crandallite groups. Many phases have been classified as members of this group depending on the occupation of the A, B, and X positions in the formula. Large cations such as Na, K, Ag, NH_4, H_3O^+, Ba, Bi, Ca, REE, Pb, Sr, Th in 12-coordination were observed in the A position, Al, Fe, Cu, Cr, V, Ga and Zn in octahedral coordination in the B position, and As, P, S, Cr and Si in the tetrahedral X anion position. A slightly different formula was proposed by Somina and Bulach (1966), in which M^{2+} and M^{3+} elements in the A position compensate the presence of (XO_3OH) group in the anion. The modified formula was presented as $(A^{2+}_{1-x}A^{3+}_x)B_3[(XO_4)_{1+x}(XO_3OH)_{1-x}(OH)_6]$. Investigation of the crandallite (Blount, 1974) and gorceixite (Radoslavich, 1982) structures indicates that the extra proton is actually attached to one of the XO_4 anions. So, the general formula may be better written as $AB_3(XO_4)(XO_3OH)(OH)_6$ (Scott 1987).

In the crandallite group, there are eight known mineral phases (arsenates and phosphates) in which Pb in the structural A position dominates (Mandarino 1999, Pring et al. 1995) (Table 1)

Up to now, crystal structures have been determined only for some members of the crandallite group. Hendricks (1937) described crystal structures of alunite and jarosite in the space group R 3m. Pabst (1947) determined alunite-type minerals in the space group R –3m and for the first time published atomic coordinates and further structural data for alunite, svanbergite and woodhouseite. Crystal structures of some minerals have been refined in this space group: goyazite and woodhouseite (Kato 1971, 1977), crandallite (Blount 1974), svanbergite (Kato – Miura 1977), beudantite (Giuseppetti – Tadini 1989), kintoreite (Kharisun et al. 1997), dussertite (Kolitsch et al. 1999a), hindsdalite and plumbogummite (Kolitsch et al. 1999c). Giuseppetti and Tadini (1987) inferred the space group R 3m for corkite and Jambor et al. (1996) for gallobeudantite. Radoslavich (1982) determined the monoclinic space group Cm for gorceixite. Szymanski (1988) estimated the space group R –3m for two crystals of beudantite and the triclinic cell for the third one.

The basic structural motive is formed in the case of the minerals of the crandallite group by octahedra with central atoms Al^{3+} and Fe^{3+}. Each octahedron shares four

Table 1 Pb dominant members (arsenates, phosphates) of crandallite group.

Fe>Al (in B site)	
kintoreite	$PbFe_3(PO_4)(PO_3OH)(OH)_6$
corkite	$PbFe_3(PO_4)(SO_4)(OH)_6$
beudantite	$PbFe_3(AsO_4)(SO_4)(OH)_6$
segnitite	$PbFe_3(AsO_4)(AsO_3OH)(OH)_6$
Al>Fe (in B site)	
plumbogummite	$PbAl_3(PO_4)(PO_3OH)(OH)_6$
hinsdalite	$PbAl_3(PO_4)(SO_4)(OH)_6$
hidalgoite	$PbAl_3(AsO_4)(SO_4)(OH)_6$
philipsbornite	$PbAl_3(AsO_4)(AsO_3OH)(OH)_6$

corners (hydroxyls) with four other adjacent octahedra. The remaining corners of each octahedron are occupied by oxygen atoms, lying in opposite sides of the plane, formed by hydroxyls. Such arrangement enables formation of a sheet built up of larger hexagonal rings and smaller trigonal ones perpendicular to the *c* axis. Cations in the A position (Pb, Ca, Sr.) lie between separate sheets in large cavities asymmetrically surrounded by six oxygens and six hydroxyls. Three oxygens in the apexes of each octahedron triad simultaneously form a basis of phosphate (arsenate, sulfate) tetrahedra. The remaining unshared oxygen of each tetrahedron points to the six-fold ring of octahedral hydroxyls (up and down towards the *c* axis – depending on the octahedra orientation) to which it is hydrogen bonded (Scharm – Scharmová 1995).

Occurrence

Cínovec

The Sn-W deposit Cínovec is located approximately 15 km north of Teplice, Krušné hory Mts., Czech republic. The vein deposit Cínovec is situated in apical part of elevation of lithium albite granite, which formed at surface irregular ellipsis with dimensions 800 x 1500 m. This "classical" vein deposit is represented by system of subhorizontal veins, which are accompanied by lateral greisenization. In 1988, during an inspection of workings mined in 1942–1944 on the vein Nr. 1, between the first and second level, there was observed a relatively rich occurrence of supergene mineralization in residual pillars (Jansa et al. 1998). Detailed description of the geological location and the rich supergene mineral association (nearly 30 mineral species), have been recently described by Jansa et al. (1998).

At Cínovec, *beudantite* was found only rarely on several samples as crystalline thin coatings and films on quartz gangue. Its color is green to greenish yellow. Beudantite forms euhedral well-formed trigonal crystals up to 50 μm in size (Fig.1). Its individual crystals grow on gangue; penetration twins (Fig. 2) and rosette aggregates (Fig. 3) are also observed.

Segnitite from Cínovec was described in detail by Jansa et al. (1998). There, it forms relatively common fine crystalline coatings (area up to 10 cm^2) in cavities of quartz gangue, and has greenish yellow to yellow green or gray yellow to brownish yellow color. These segnitite coatings are growing to opal or stolzite crust and close wulfenite crystals at some places, too. The barium-pharmacosiderite coatings are the youngest minerals in this association.

Philipsbornite was found at Cínovec only on some samples as grayish to yellowish green thin coatings on "wood" cassiterite and as fillings of tiny cavities of quartz gangue. As a rule, cassiterite is first coated by opal, stolz-

Fig. 1 Scanning electron micrograph of euhedral trigonal crystals of beudantite from Cínovec (ESM Tesla BS 340, photo by I. Čejková and J. Sejkora, National Museum, Prague).

Fig. 2 Scanning electron micrograph of penetration twins of beudantite from Cínovec (ESM Tesla BS 340, photo by I. Čejková and J. Sejkora, National Museum, Prague).

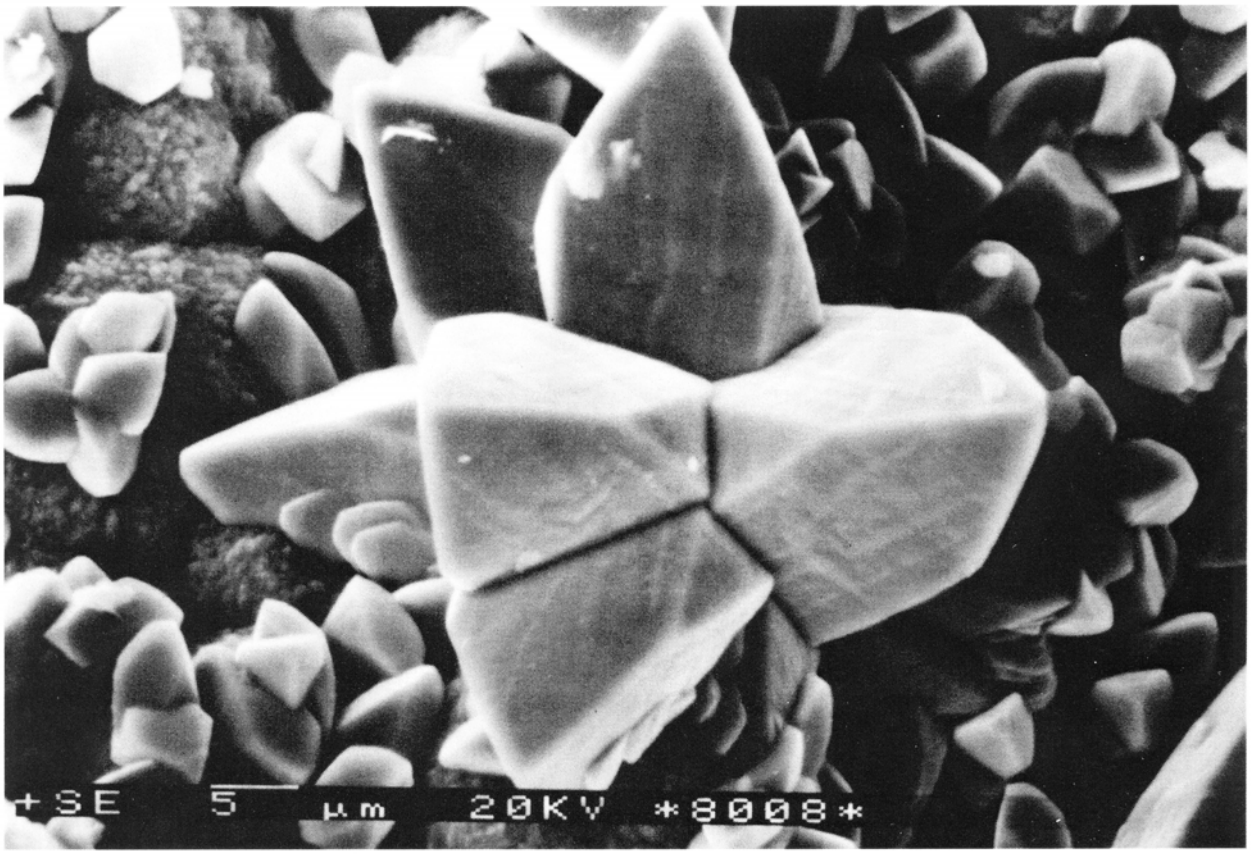

Fig. 3 Scanning electron micrograph of rosette aggregate of beudantite from Cínovec (ESM Tesla BS 340, photo by I. Čejková and J. Sejkora, National Museum, Prague).

ite follows as a next phase and philipsbornite represents the youngest mineral in this association. Very thin isometric crystals (up to 4–9 μm in size) were observed sporadically on the surface of its irregular coatings (David et al. 1990).

Moldava

The studied samples were found at the Moldava deposit, Krušné hory Mts. (Czech Republic). The mining district Moldava is located approximately 20 km northwest of Teplice and is represented by two main fluorite–barite–quartz veins, Josef and Papoušek, which are the largest among similar veins occurring in the crystalline rocks of the Krušné hory Mts.

The fluorite-quartz-barite veins with NW-SE direction can be traced for about 5 km. They were verified in depth of 700 m below the surface by bore holes. The thickness of veins is usually 2–3 m, locally increases to 6 m. The wallrock of veins is composed of various ortho- and paragneisses as well as granitoide. The vein-filling is massive or displays cavities filled with green, yellow a violet fluorite crystals. Later on, occasional small stringers of galena, Ni-skutterudite, rammelsbergite, safflorite, marcasite, proustite, tennantite, native silver and bismuth are observed.

Under weathering conditions, these primary ore minerals have been partially oxidized, leading to a very rich assemblage of supergene minerals, predominately arsenates and sulfates. The oxidation zone was discovered in 1968 at the fifth level of the Josef shaft (150 m below the surface) and continued up to the 7th level at the depth of 300 m (Fengl 1982). Mineralogy of the weathering zone in vein Josef was studied by Fengl et al. (1981) and more recently by Sejkora and Řídkošil (1994) and Sejkora et al. (1994, 1998).

Two samples of *beudantite* from Moldava were studied. In both cases, beudantite occurs in strongly supergene altered fluorite gangue (colorless, white and violet). The sample (A) of beudantite forms fillings of small cavities (up to 0.5 cm) and crystalline coatings and earthy to compact crusts. It has yellowish brown color. Its surface is formed by tiny (up to 10 μm in size) trigonal crystals (Figs 4, 5). The beudantite (B) sample was found as olive brown compact crusts (thickness up to 3 mm) in cavities (up to 1 cm in size) of fluorite gangue. These crusts have greasy to vitreous luster and reniform to globular smooth surface. In close association with both samples, mimetite and cerussite were observed.

At Moldava, *segnitite* forms fillings of small cavities in strongly supergene altered fluorite gangue and crusts (thickness 0.5–2 mm) in larger cavities (up to 1.5 cm) with reniform to globular surface. Surface of crusts is usually smooth, only occasionally trigonal crystals with size in the range 3–40 μm (Figs 6, 7) were observed. Segnitite crusts have dark green to greenish black color and

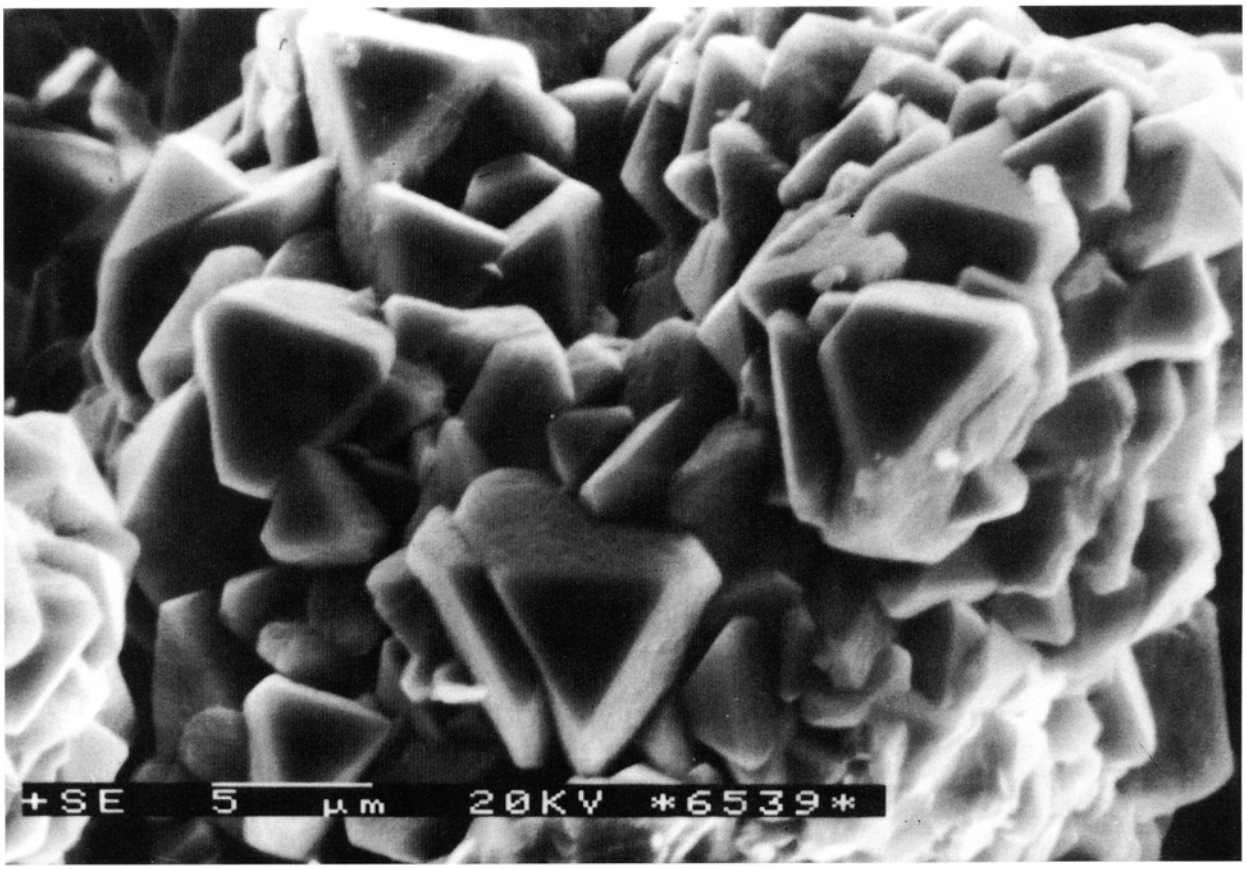

Fig. 4 Scanning electron micrograph of groups of trigonal crystals of beudantite from Moldava (ESM Tesla BS 340, photo by I. Čejková and J. Sejkora, National Museum, Prague).

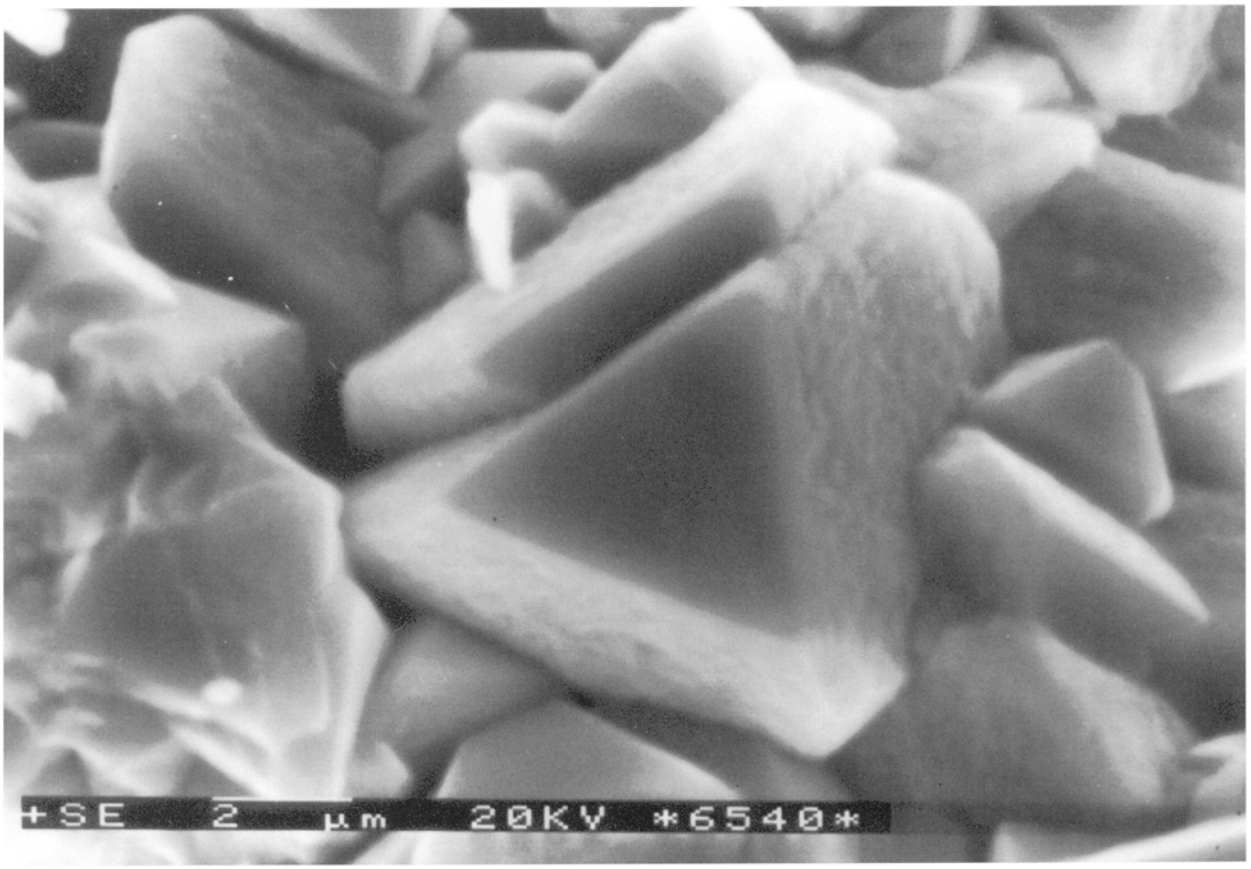

Fig. 5 Scanning electron micrograph of trigonal crystals of beudantite from Cínovec (ESM Tesla BS 340, photo by I. Čejková and J. Sejkora, National Museum, Prague).

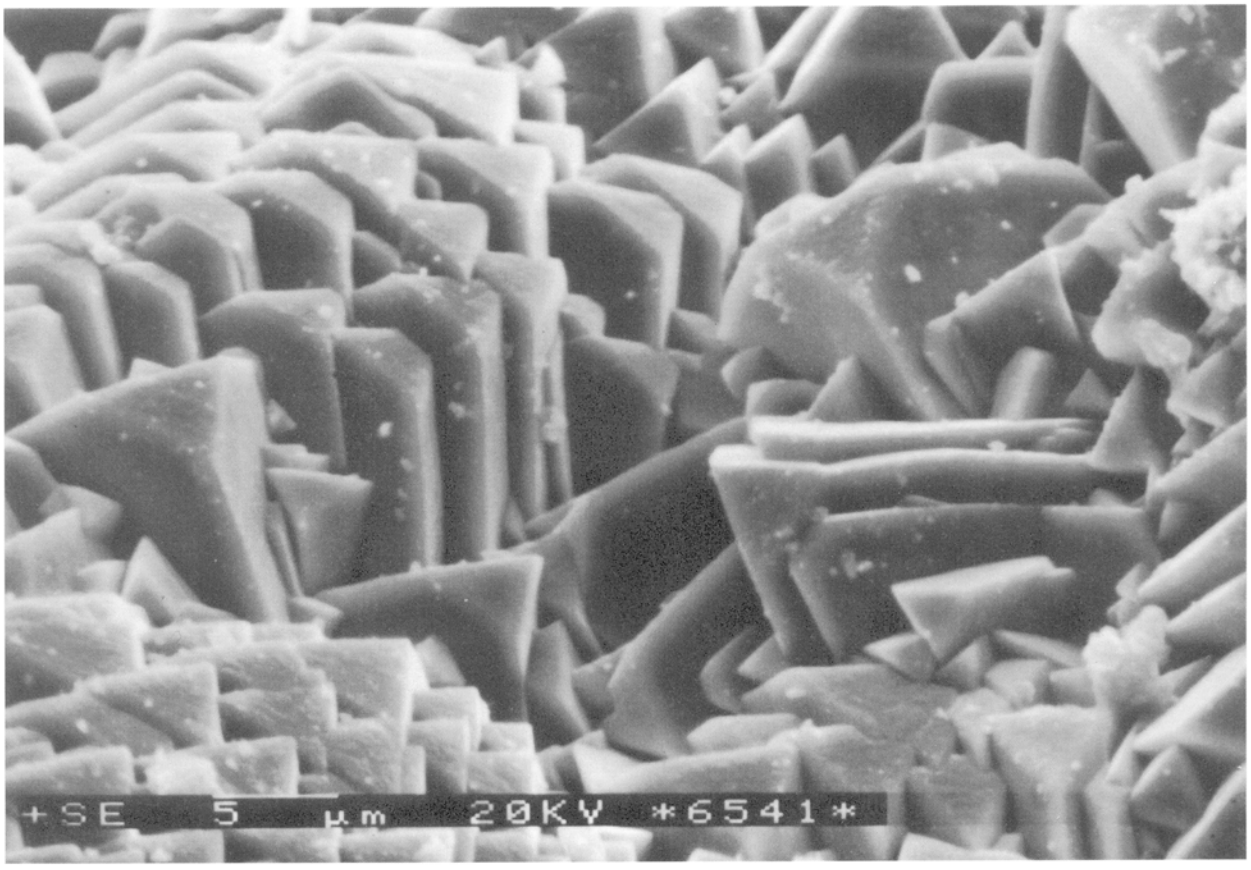

Fig. 6 Scanning electron micrograph of surface of segnitite crusts from Moldava (ESM Tesla BS 340, photo by I. Čejková and J. Sejkora, National Museum, Prague).

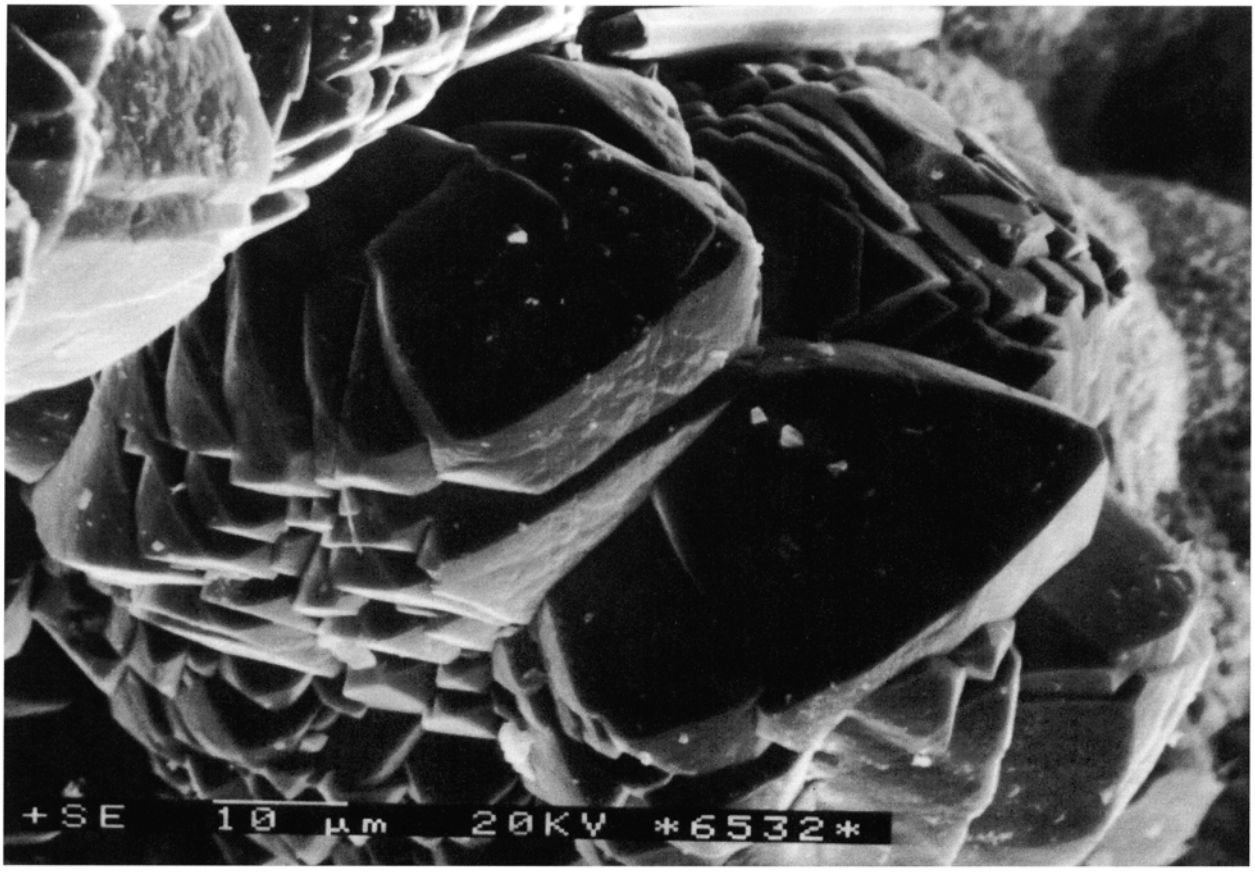

Fig. 7 Scanning electron micrograph of groups of trigonal crystals of segnitite from Moldava (ESM Tesla BS 340, photo by I. Čejková and J. Sejkora, National Museum, Prague).

greasy to vitreous luster. Mimetite, phosphatian mimetite and cerussite were determined in close association.

Philipsbornite has been found at Moldava only very rarely as grayish to apple green fine grained aggregates on mimetite and fluorite. The size of these aggregates reaches 10 x 20 x 1 mm. Its luster is greasy, fracture uneven and cleavage was not observed. It is associated with mimetite, thometzekite, mawbyite and other Cu-Pb minerals (Sejkora et al. 1998).

At Moldava, *plumbogummite* was found in the form of blue to bluish gray fine grained aggregates (up to 3 cm) in the cavity of quartz. Fluorite gangue. It has greasy to vitreous luster and no cleavage. The surface of plumbogummite aggregates is composed of fine lenticular to spherical aggregates up to 1 mm in size (Fig. 8). The sometimes hollow aggregates (Fig. 9) probably present pseudomorphs from crystals of pyromorphite and are formed of up to 10 mm large perfectly developed trigonal crystals. Plumbogummite is associated with wulfenite, pyromorphite, phosphatian mimetite, duftite and cerussite (Sejkora et al. 1998).

X-ray powder diffraction data

X-ray powder diffraction patterns (Table 2) were obtained from a hand-picked samples using the diffractometers HZG4/TuR and DRON 3 (CuKα and CoKα radiation, step-scanning). To minimize complicated shape of background due to classic glass sample holder, the sample studied was placed on the surface of flat silicon wafer from alcoholic suspension. Positions and intensities of reflections were calculated using Pearson VII profile shape function by ZDS program package (Ondruš 1995). In order to index the powder diffraction patterns, information on crystal structures of each mineral phases was used to generate the theoretical powder data by the Lazy Pulverix program (Yvon et al. 1977). The lattice parameters of studied mineral phases (Table 3 and 4) in following text were calculated by the least-squares refinement program of Burnham (1962).

The a/c diagram in Fig. 10 was constructed using unit cell dimensions of the minerals studied together with those published for other Pb dominant members of the crandallite family (Lengauer et al. 1994 and others). In this a/c diagram, As, P and Al, Fe members of this family fill limited fields. This fact demonstrates the possibility to distinguish these mineral phases on the basis of their lattice unit cell parameters. Fe^{3+} or Al^{3+} content in the B position of the general formula is manifested with a difference in the parameter *a* in the range 0.2–0.3 Å, which agrees with ion radii Fe^{3+} (0.64 Å) and Al^{3+} (0.51 Å) (Scott 1987). The lattice parameter *c* is influenced especially by As-P substitution in the (XO_4) site of the general formula. A substitution of P in the tetrahedron (average bond length 1.56 Å – Scott 1987) by As (1.78 Å) causes an increase in the *c* parameter by about

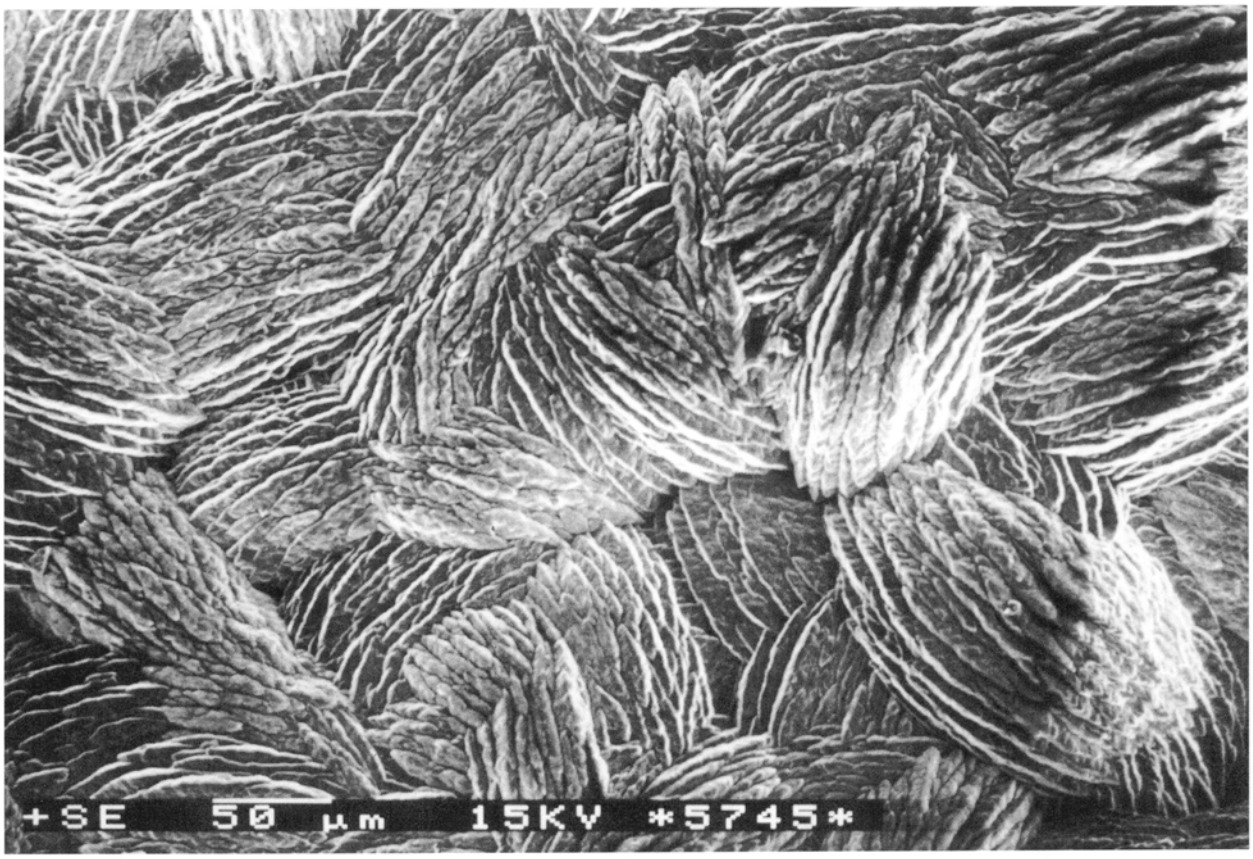

Fig. 8 Scanning electron micrograph of aggregates of plumbogummite from Moldava (ESM Tesla BS 340, photo by I. Čejková and J. Sejkora, National Museum, Prague).

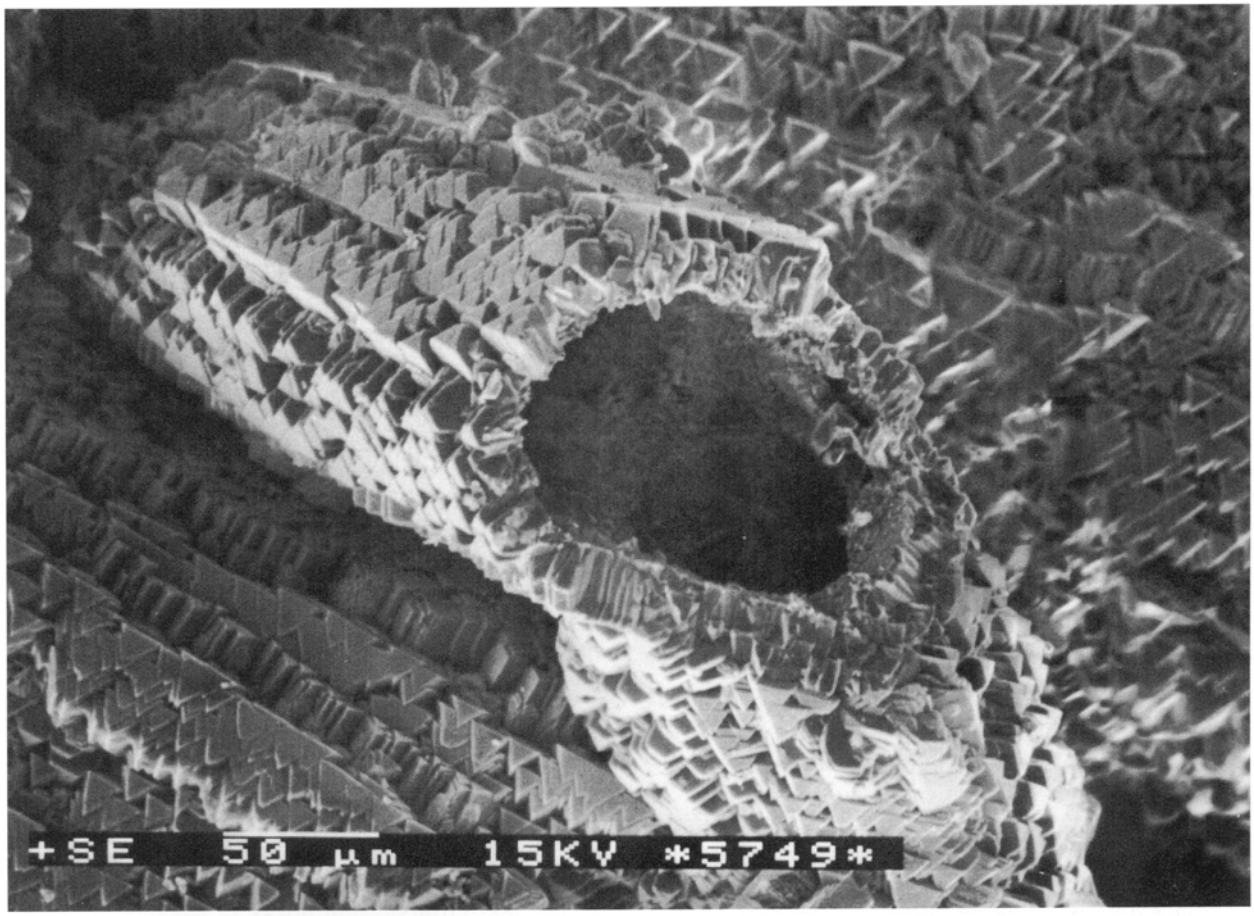

Fig. 9 Scanning electron micrograph of surface of aggregates of plumbogummite from Moldava (ESM Tesla BS 340, photo by I. Čejková and J. Sejkora, National Museum, Prague).

Table 2 X-ray powder diffraction data for samples studied.

			beudantite Cínovec*1			segnitite Moldava*2			beudantite (B) Moldava*3			beudantite (A) Moldava*4		
h	k	l	d_{obs}	I/I_o	d_{calc}	d_{obs}	I/I_o	d_{calc}	d_{obs}	I/I_o	d_{calc}	d_{obs}	I/I_o	d_{calc}
1	0	1	5.980	37	5.980	5.990	34	5.980	5.970	77	5.960	5.960	66	5.960
1	0	4	5.710	9	5.690	5.710	10	5.700	5.670	16	5.680	5.670	10	5.670
1	1	0	3.685	47	3.686	3.689	66	3.687	3.675	89	3.675	3.671	49	3.673
1	0	4	3.549	24	3.549	3.555	24	3.553	3.564	20	3.539	3.533	10	3.536
1	1	3	3.094	100	3.094	3.098	100	3.096	3.085	100	3.085	3.083	100	3.083
1	1	–3			3.094			3.096			3.085			3.083
2	0	2	2.990	35	2.990	2.992	36	2.991	2.982	20	2.981	2.978	16	2.979
0	0	6	2.847	36	2.846	2.854	36	2.851	2.836	27	2.838	2.835	19	2.835
0	2	4	2.556	27	2.556	2.560	33	2.558	2.548	15	2.549	2.546	14	2.547
1	2	–1	2.389	18	2.389	2.389	30	2.390	2.381	14	2.382	2.380	7	2.381
2	1	1			2.389			2.390			2.382			2.381
2	1	–2	2.324	16	2.322	2.323	30	2.323	2.316	16	2.315	2.316	11	2.314
1	2	2			2.322			2.323			2.315			2.314
1	0	7	2.278	35	2.279	2.283	38	2.283	2.272	21	2.272	2.271	14	2.270
1	1	6	2.253	20	2.253	2.257	31	2.255	2.245	12	2.246	2.243	8	2.244
1	1	–6			2.253			2.255			2.246			2.244
3	0	0	–			2.129	28	2.128	2.121	17	2.122	2.121	11	2.121
1	2	–4	–			2.101	28	2.102	2.101	14	2.095	2.097	10	2.093
2	1	4	–					2.102			2.095			2.093
3	0	3	1.9931	36	1.9932	1.9948	52	1.9940	1.9869	27	1.9876	1.9858	23	1.9862
0	3	3			1.9932			1.9940			1.9876			1.9862
2	1	–5	1.9698	13	1.9706	1.9701	3	1.9722	1.9631	6	1.9651	1.9622	4	1.9636
1	2	5			1.9706			1.9722			1.9651			1.9636
2	2	0	1.8424	29	1.8428	1.8438	55	1.8433	1.8373	30	1.8377	1.8363	14	1.8364
2	1	7	1.7155	14	1.7154	1.7149	31	1.7172	–			–		
1	2	–7			1.7154			1.7172	–			–		
1	1	9	1.6867	19	1.6869	1.6894	34	1.6895	1.6817	8	1.6822	1.6801	6	1.6807
1	1	–9			1.6869			1.6895			1.6822			1.6807
2	2	6	1.5465	19	1.5469	1.5486	35	1.5480	1.5422	8	1.5425	1.5409	8	1.5414
2	2	–6			1.5469			1.5480			1.5425			1.5414
0	2	10	1.5060	14	1.5057	1.5085	32	1.5079	1.5015	6	1.5014	1.5017	6	1.5001

*1 Diffractometer HZG 4, CuKα radiation, step scanning 0.05 °2θ/6 sec., measured range 12–64 °2θ.
*2 Diffractometer HZG 4, CuKα radiation, step scanning 0.05 °2θ/6 sec., measured range 10–70 °2θ.
*3 Diffractometer DRON 3, CoKα radiation, step scanning 0.02 °2θ/3 sec., measured range 10–78 °2θ.
*4 Diffractometer DRON 3, CoKα radiation, step scanning 0.02 °2θ/3 sec., measured range 10–78 °2θ.

Table 3 Unit cell parameters for Pb and Fe dominant members of the crandallite group (for trigonal R 3m or R –3m space group).

	occurrence		A	B	X	a	c	c/a	V
segnitite	Moldava	this paper	Pb	Fe	As	7.373(1)	17.108(4)	2.320	805.4(2)
segnitite	Cínovec	Jansa et al. (1998)	Pb	Fe	As	7.348(3)	17.09(1)	2.326	799.1
segnitite	Broken Hill	Birch et al. (1992)	Pb	Fe	As	7.359(3)	17.113(8)	2.326	802.6
segnitite	St. Andreasberg	Bischoff (1999)	Pb	Fe	As	7.376(1)	17.145(2)	2.324	807.8
segnitite	Pützbach, Bad Ems	Bischoff (1999)	Pb	Fe	As	7.364(1)	17.145(4)	2.328	805.2
beudantite	Cínovec	this paper	Pb	Fe	As, S	7.3713(9)	17.076(2)	2.317	803.5(1)
beudantite	Moldava (A)	this paper	Pb	Fe	As, S	7.346(1)	17.012(5)	2.316	795.0(3)
beudantite	Moldava (B)	this paper	Pb	Fe	As, S	7.351(2)	17.028(8)	2.316	796.8(5)
beudantite	Dernbach	Giuseppetti, Tadini (1987)	Pb	Fe	As, S	7.337	17.034	2.322	794.1
beudantite	Tsumeb	Szymanski (1988)	Pb	Fe	As, S	7.3151(9)	17.0355(5)	2.329	789.5

Table 4 Unit cell parameters for Pb and Al dominant members of crandallite group (for trigonal R 3m or R –3m space group).

	occurrence		A	B	X	a	c	c/a	V
philipsbornite	Moldava	Sejkora et al (1998)	Pb	Al	As	7.073(7)	17.14(3)	2.423	742.6
philipsbornite	Cínovec	David et al. (1990)	Pb	Al	As	7.14	17.13	2.399	756.3
philipsbornite	Tsumeb	Schmetzer et al. (1982)	Pb	Al	As	7.174	17.18	2.395	765.7
philipsbornite	Dundas	Walenta et al. (1982)	Pb	Al	As	7.11	17.05	2.398	796.4
plumbogummite	Moldava	Sejkora et al. (1998)	Pb	Al	P	7.023(7)	16.97(7)	2.416	724.9
plumbogummite	Reichenbach	Kolitsch et al. (1999)	Pb	Al	P	7.039(5)	16.761(3)	2.381	719.2(7)

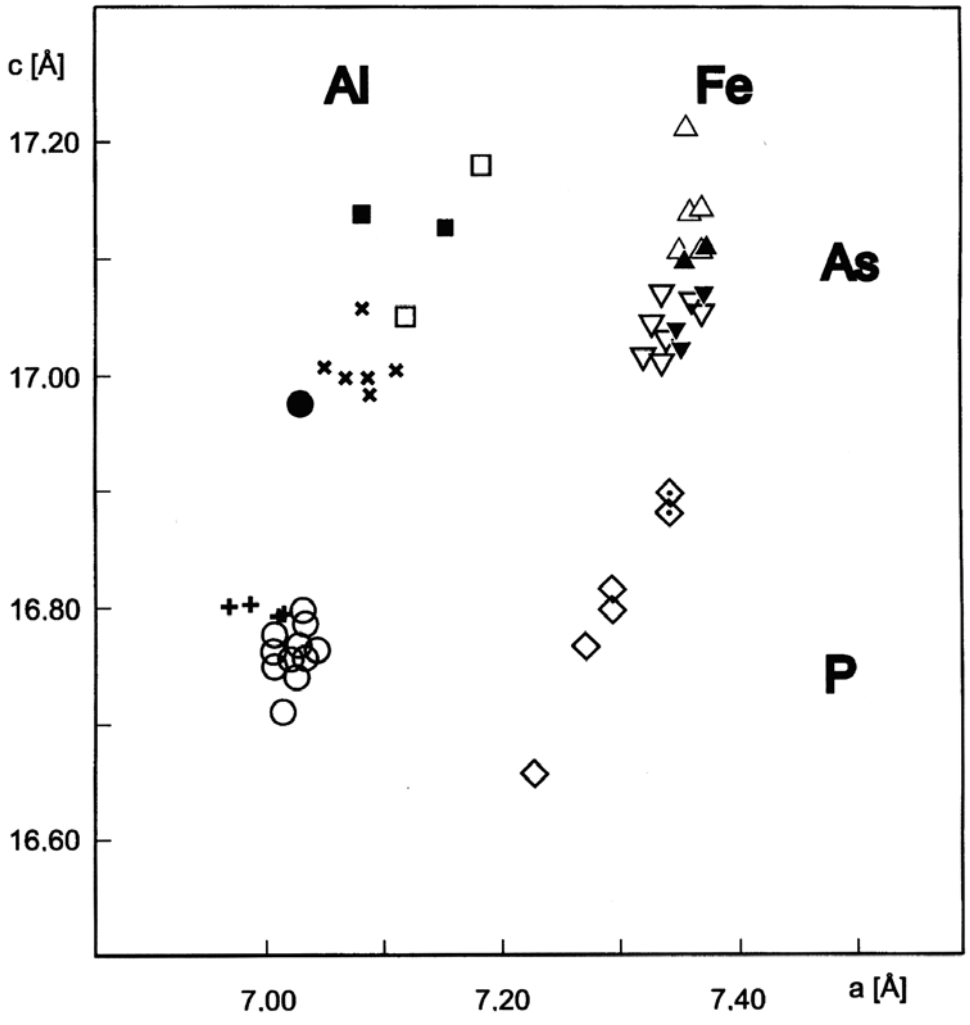

Fig. 10 The a/c plot for Pb dominant members of crandallite group. ● – plumbogummite (this paper), ○ – plumbogummite, + – hinsdalite, × – hidalgoite, ■ – philipsbornite (this paper), □ – philipsbornite, ▼ – beudantite (this paper), ∇ – beudantite, ▲ – segnitite (this paper), Δ – segnitite, ◈ – kintoreite, ◇ – corkite.

0.2–0.4 Å. The presence of $(SO_4)^{2-}$ ions (1.55 Å, Jambor et al. 1996) influences the lattice parameters less than other anions (Sejkora et al. 1998). The unit cell parameters of samples studied are in good agreement with other published data (Fig. 10). The arsenatian plumbogummite from Moldava is an exception; it occupies a position between the fields belonging to plumbogummite (P) and philipsbornite (As) in the diagram.

Chemical composition

Quantitative chemical analyses were carried out by means of JEOL JXA-50A electron microprobe in an energy dispersive mode (EDAX PV 9400, performed by V. Šrein and A. Langrová), operated at an acceleration potential 30 kV, a sample current $5.7 \cdot 10^{-10}$ A and 1–2 μm electron beam size. The reported H_2O percentages for each specimen were calculated on the basis of valence balance in the proposed general formula $AB_3(XO_4)(XO_3OH)(OH)_6$ or $AB_3(XO_4)(SO_4)(OH)_6$, respectively. Empirical formulae were calculated on the basis of six atoms (1 in the A position, 3 in the B position, 2 in the X position) and recalculated on the sum $(AsO_3OH) + (SO_4) = 1.00$ Chemical composition of the minerals studied agrees with the stoichiometry (Tables 5 and 6).

Two samples of *beudantite* from *Moldava* were analyzed: sample (A) – moderately zoned beudantite with sulfate content in the range 35–50 mol. %, (Fig. 11). Empirical "average" formula (mean of 4 point analyses):
$(Pb_{1.06}Ba_{0.03})_{\Sigma}S_{1.09}(Fe_{2.77}Al_{0.12}Cu_{0.05}Sb_{0.02})_{\Sigma 2.96}(AsO_4)_{0.85}(AsO_3OH)_{0.18}(SO_4)_{0.82}(PO_4)_{0.10}(OH)_{6.18}$

sample (B) has strongly zonal composition: middle of aggregates is formed by beudantite with 48 mol. % sulfate, sulfate content gradually decreases and margin zone is composed by segnitite with only 16 mol. % sulfate. Empirical formula, which represents hypothetical "average" composition of this sample (mean of 3 point analyses) is
$(Pb_{1.06}Ba_{0.02})_{\Sigma 1.08}(Fe_{2.81}Al_{0.08}Cu_{0.07}Sb_{0.02})_{\Sigma 2.98}(AsO_4)_{0.85}(AsO_3OH)_{0.37}(SO_4)_{0.63}(PO_4)_{0.09}(OH)_{6.21}$.

Beudantite from *Cínovec* is relatively strongly zoned (Fig. 12) – middle of crystals is represented by beudantite with up to 47 mol. % sulfate, sulfate content decreases to the margin and the marginal part is formed by segnitite with only 23 mol. % sulfate. Empirical formula, which represents hypothetical "average" composition of this sample, may be expressed (mean of 6 point analyses) as
$(Pb_{1.06}Ba_{0.02})_{S1.08}(Fe_{2.72}Al_{0.11}Cu_{0.05}In_{0.04}Sb_{0.03})_{S2.95}(AsO_4)_{0.86}(AsO_3OH)_{0.33}(SO_4)_{0.67}(PO_4)_{0.10}(OH)_{6.08}$.

Table 5 Chemical composition of segnitite from Moldava and Cínovec.

		Moldava	Cínovec*1	Cínovec*2	*3
	mean		mean	mean	
As_2O_5	27.10	26.66–27.74	30.7	24.6	30.42
Al_2O_3	0.65	0.09– 1.18	2.3	0.5	
P_2O_5	0.79	0.33– 1.32	–	0.7	
SO_3	1.58	1.11– 1.90	–	4.1	
PbO	32.24	31.46–32.95	30.7	30.6	29.54
Sb_2O_5	0.93	0.64– 1.32	–	–	
BaO	0.48	0.00– 1.06	0.6	–	
Fe_2O_3	27.11	25.74–27.68	26.1	30.5	31.70
CuO	1.92	1.52– 2.11	1.4	0.8	
H_2O*	6.72		6.9	7.1	8.35
total	99.52		98.70	98.90	100.00
As	1.776		2.011	1.579	2.000
Al	0.096		0.332	0.072	
P	0.084			0.073	
S	0.148			0.378	
Pb	1.091		1.036	1.010	1.000
Sb	0.043				
Ba	0,024		0.027		
Fe	2.557		2.461	2.818	3.000
Cu	0.181		0.133	0.070	

*1 sulfate free segnitite from Cínovec (Jansa et al. 1998)
*2 segnitite from Cínovec (Jansa et al. 1998)
*3 theoretical composition of segnitite – $PbFe_3(AsO_4)(AsO_3OH)(OH)_6$
H_2O* – content of H_2O calculated on the basis on valence balance

The observed indium contents are remarkable to a large extent, which reach up to 2.44 wt. % In_2O_3 in the marginal parts of the crystals studied. The indium contents in the minerals of the crandallite group have not yet been published. The finding of In-containing beudantite for Cínovec may be probably related to a certain indium amount mobilized during supergene process of roquesite. Novák et al. (1995) described also a rare mineral dzhalindite $In(OH)_3$, of the same association as beudantite studied in this paper.

Segnitite from *Moldava* is relatively homogeneous – its empirical formula (mean from 8 point analysis) is:
$(Pb_{1.09}Ba_{0.02})_{\Sigma 1.11}(Fe_{2.56}Cu_{0.18}Al_{0.10}Sb_{0.04})_{\Sigma 2.88}(AsO_4)_{0.93}$
$(AsO_3OH)_{0.85}(SO_4)_{0.15}(PO_4)_{0.08}(OH)_{5.61}$.

According to Jansa et al. (1998), two segnitite types may be characterized from *Cínovec*, i.e. the dominant phase not containing sulfate ions with somewhat higher Al content, the empirical formula of its being
$(Pb_{1.04}Ba_{0.03})_{S1.07}(Fe_{2.46}Cu_{0.13}Al_{0.33})_{S2.92}(AsO_4)_{1.01}$
$(AsO_3OH)_{1.00}(OH)_{5.74}$,

and the more rare sulfate rich segnitite, possessing the empirical formula
$Pb_{1.01}(Fe_{2.82}Cu_{0.07}Al_{0.07})_{S2.96}(AsO_4)_{0.95}(AsO_3OH)_{0.63}$
$(SO_4)_{0.37}(PO_4)_{0.07}(OH)_{5.77}$.

This segnitite may be, according our classification, related to beudantite and represents a transition form to sample analyzed by us.

Philipsbornite from *Cínovec* (David et al. 1990) is practically a pure As member with only minimum sulfate and phosphate content. Certain contents of Ba in the A position and Fe in the B position of general formula were described. Empirical formula:
$(Pb_{0.78}Ba_{0.20}Bi_{0.02})_{\Sigma 1.00}(Al_{2.46}Fe_{0.48}Cu_{0.03})_{\Sigma 2.97}\ (AsO_4)_{1.98}$
$(PO_4)_{0.02}(SO_4)_{0.01}(OH)_{4.88} \cdot 1.06H_2O$.

For *philipsbornite* from *Moldava* (Sejkora et al. 1998), 11 mol. % of $(SO_4)^{2-}$ and 9 mol. % of $(PO_4)^{3-}$ components in X position are characteristic.

Empirical formula (mean from two point analyses):
$(Pb_{1.05}Ca_{0.01}Bi_{0.03})_{\Sigma 1.09}(Al_{2.91}Fe_{0.12})_{\Sigma 3.03}$
$[(As_{1.18}P_{0.13}O_4)_{\Sigma 1.31}(As_{0.40}P_{0.04}O_3$
$OH)_{\Sigma 0.44}(SO_4)_{0.22}]\ (OH)_6$.

Arsenatian *plumbogummite* from *Moldava* (Sejkora et al. 1998) is practically sulfate free and approximately 32 mol. % of the $(AsO_4)^{3-}$ (philipsbornite) component are present.

Empirical formula (mean from two point analyses):
$(Pb_{1.03}Ca_{0.03})_{\Sigma 1.06}Al_{2.94}[(P_{0.54}As_{0.25}O_4)_{\Sigma 0.79}$
$(P_{0.86}As_{0.40}O_3OH)_{\Sigma 1.26}\ (SO_4)_{0.01}]\ (OH)_6$.

Individual point analyses for all phases mentioned were plotted in the diagrams for Pb-Fe (Fig. 13) and Pb-Al (Fig. 14) dominant members of crandallite group. The classification

Table 6 Chemical composition of beudantite from Moldava and Cínovec.

	Moldava (A)		Moldava (B)		Cínovec		*1
	mean	range	mean	range	mean	range	
As_2O_5	19.48	15.21–24.13	16.63	13.93–19,01	18.49	15.53–24.15	16.15
Al_2O_3	0.54	0.27– 0.91	0.86	0.45– 1.26	0.77	0.00– 1.34	
P_2O_5	0.87	0.21– 1.34	0.97	0.19– 1.46	0.94	0.34– 1.66	
SO_3	7.03	3.50–10.09	9.27	7.14–10.81	7.23	5.11– 9.86	11.25
PbO	32.87	31.60–33.74	33.15	32.73–34.05	32.08	29.68–33.93	31.36
Sb_2O_5	0.54	0.48– 0.64	0.47	0.21– 0.59	0.68	0.39– 1.29	
BaO	0.32	0.13– 0.46	0.55	0.35– 0.72	0.35	0.00– 0.71	
Fe_2O_3	31.13	29.31–32.54	31.07	29.66–32.51	29.34	25.57–32.04	33.65
CuO	0.74	0.63– 0.81	0.56	0.18– 0.84	0.57	0.21– 0.89	
In_2O_3	–		–		0.81	0.00– 2.44	
H_2O*	7.72		7.85		7.40		7.60
total	101.24		101.38		98.66		100.00
As	1.222		1.030		1.191		1.000
Al	0.076		0.120		0.111		
P	0.088		0.097		0.098		
S	0.633		0.825		0.669		1.000
Pb	1.062		1.058		1.064		
Sb	0.024		0.020		0.031		
Ba	0.015		0.026		0.017		
Fe	2.813		2.772		2.721		3.000
Cu	0.067		0.050		0.053		
In	–		–		0.043		

*1 theoretical composition of beudantite – $PbFe_3(AsO_4)(SO_4)(OH)_6$
H_2O* – content of H_2O calculated on the basis on valence balance

proposed by Novák et al. (1994) for the crandallite group minerals with Pb dominant in the A position has been applied for ternary diagrams construction.

At present, it is clear, the isomorphism in the minerals of crandallite group seems to be very extensive in all three positions of the general formula $AB_3(XO_4)(XO_3OH)$. or $AB_3(XO_4)(SO_4)$.

For all studied samples, Pb is highly dominant in the A position. The Ca, Ba and Bi contents (with exception of philipsbornite sample from Cínovec) observed are very low. Practically, complete isomorphism in the A position has been well known for a long time. Complete isomorphism of Fe-Al in the B position was described by Brophy et al. (1962), Jambor and Dutrizac (1983) and Scott (1987). On the contrary, Rattray et al. (1996) found only very limited Fe-Al substitution at samples from Broken Hill, Australia. Recently Jambor et al. (1996) described the mineral gallobeudantite containing a dominant amount of Ga in the B position; the springcreekite phase studied by Kolitsch et al. (1999b) contains V^{3+}. The not yet described indium content (beudantite, Cínovec) inferred from the minorities in the B position in the structure of our samples studied seems to be the most interesting. Some Cu (for example Rattray et al. 1996) and Sb (dussertite, Kolitsch et al. 1999a) containg samples have been also described.

The (XO_4) position isomorphism has been described only recently (Scott 1987, Birch et al. 1992, Pring et al. 1995, Rattray et al. 1996, Kharisun et al. 1997), its broad extent for Pb dominant members with prevalence of Al^{3+} and Fe^{3+} in the B position is evident from Figs 13 and 14.

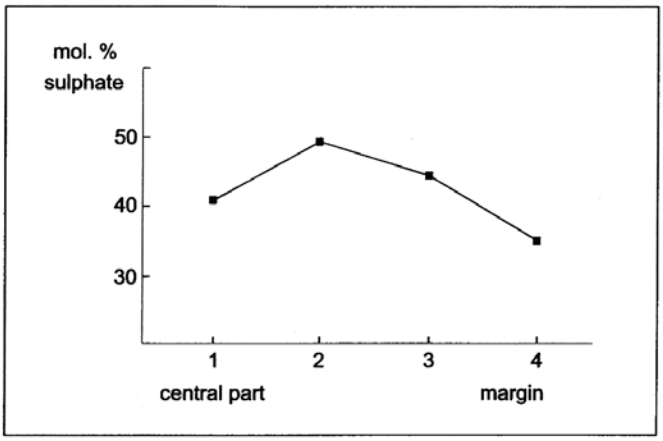

Fig. 11 The graph of chemical composition of zoned beudantite (A) from Moldava.

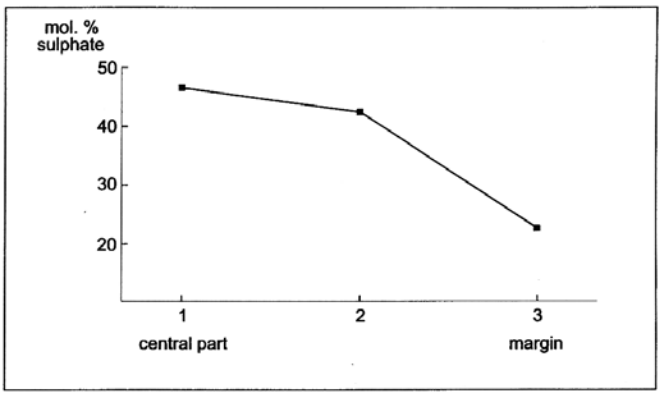

Fig. 12 The graph of chemical composition of zoned beudantite from Cínovec.

Infrared absorption spectroscopy

An assignment and interpretation of the infrared spectra of the mineral phases studied make problems because of possible coincidences of anion skeletal vibrations. This interpretation has been done with regard on some available infrared and Raman spectroscopical data (e. g. Keller 1971; Farmer 1974; Gevorkyan et al. 1976, Myneni et al. 1998, Sasaki et al. 1998, Liferovich et al. 1999). The T_d symmetry of $(AsO_4)^{3-}$ is rarely preserved in the natural samples because of the arsenate anion strong affinity to protonate, hydrate and complex with metals (Myneni et al. 1998).

Infrared spectra of beudantite (from Cínovec), segnitite and arsenatian plumbogummite (both from Moldava) samples were measured with the FTIR Nicolet 740 type apparatus (absorption spectrum of the mineral phase dispersed in KBr disk).

Bands observed in the 3600–2000 cm^{-1} region were tentatively assigned to the ν OH stretching vibrations related to hydroxyls and molecular water, and ν PO_3-OH and probably to ν AsO_3OH vibrations (Tables 7–9). The presence of molecular water is confirmed by δ H_2O bending vibrations in the 1600 cm^{-1} region (beudantite 1634 cm^{-1}; segnitite 1632 cm^{-1}; plumbo-gummite 1656 and 1619 cm^{-1}). In the case of plumbogummite, two structurally nonequivalent types of water molecules in the structure may be inferred from the sharp band at 1656 cm^{-1} and a shoulder at 1619 cm^{-1}. This is in agreement with thermogravimetric analysis of plumbogummite (Sejkora et al. 1998). Lowering of the wavenumbers of ν OH stretching vibrations, broad character of bands in the 3300–3200 cm^{-1} region, and increasing of wavenumbers of δ H_2O vibrations support existence of hydrogen bonding networks in all mineral structures studied. It does not seem probable that these structures may contain free hydroxyls not participating in hydrogen bonding networks.

Weak bands and shoulders observed in the range 1500–1100 cm^{-1} may be assigned to δ P-OH and/or δ As-OH in-plane bending vibrations (beudantite 1235 cm^{-1}; segnitite 1434, 1277, 1214, 1162 cm^{-1}; plumbogummite 1496, 1414, 1281, 1182 cm^{-1}). Some coincidences with overtones and/or combination bands are possible. In the case of beudantite, however, a very strong band at 1100 cm^{-1} and shoulders at 1169 and 1235 cm^{-1}, and in the case of segnitite a strong band at 1090 cm^{-1}, weak bands at 1277 and 1214 cm^{-1} and a shoulder at 1162 cm^{-1} may be assigned to the ν_3 SO_4 antisymmetric stretching vibrations. Two sharp bands at 1100 and 1029 cm^{-1} and

a shoulder at 1182 cm^{-1} observed in the infrared spectrum of plumbogummite may be connected with the ν_3 PO_4 and ν_3 PO_3 antisymmetric triply degenerate stretching vibrations. There may be some coincidences of the ν_3 PO_4 antisymmetric stretching vibrations at 1029 cm^{-1}. However, an assignment of shoulders at 1035 cm^{-1} (beudantite) and 1024 cm^{-1} (segnitite) may relate to the δ As-OH in-plane bending vibrations. A shoulder at 999 cm^{-1} (beudantite) and 995 cm^{-1} (segnitite) may be connected with the ν_1 SO_4 symmetric stretching vibrations.

A band at 803 cm^{-1} with a shoulder at 854 cm^{-1} (beudantite), and bands at 802 and 849 cm^{-1} (segnitite) may be assigned to the ν_3 AsO_4 antisymmetric triply degenerate stretching vibrations and ν_1 AsO_4 symmetric stretching vibration, respectively. However, there may be a coincidence with the d As-OH out-of-plane bending vibration. For plumbogummite, a broad band at 851 cm^{-1} may be assigned to the ν_3 AsO_4 antisymmetric triply degenerate stretching vibration and a shoulder at 784 cm^{-1} to the ν_1 AsO_4 symmetric stretching vibration and/or δ P-OH out-of-plane bending vibration. Bands at 687 and 621 cm^{-1} (beudantite) are assigned to the n_4 SO_4 triply degenerate bending vibration, however, there may be a coin-cidence with d As-OH bending vibration and/or ν As--OH stretching vibration. In the infrared spectrum of segnitite, a band at 690 cm^{-1} may be assigned to the ν As-OH stretching vibration, bands at 621 and 523 cm^{-1} to the δ As-OH out-of-plane bending vibrations. Some coincidences of the ν_4 SO_4 triply degenerate bending vibrations and the ν As-OH stretching vibration at 690 cm^{-1}

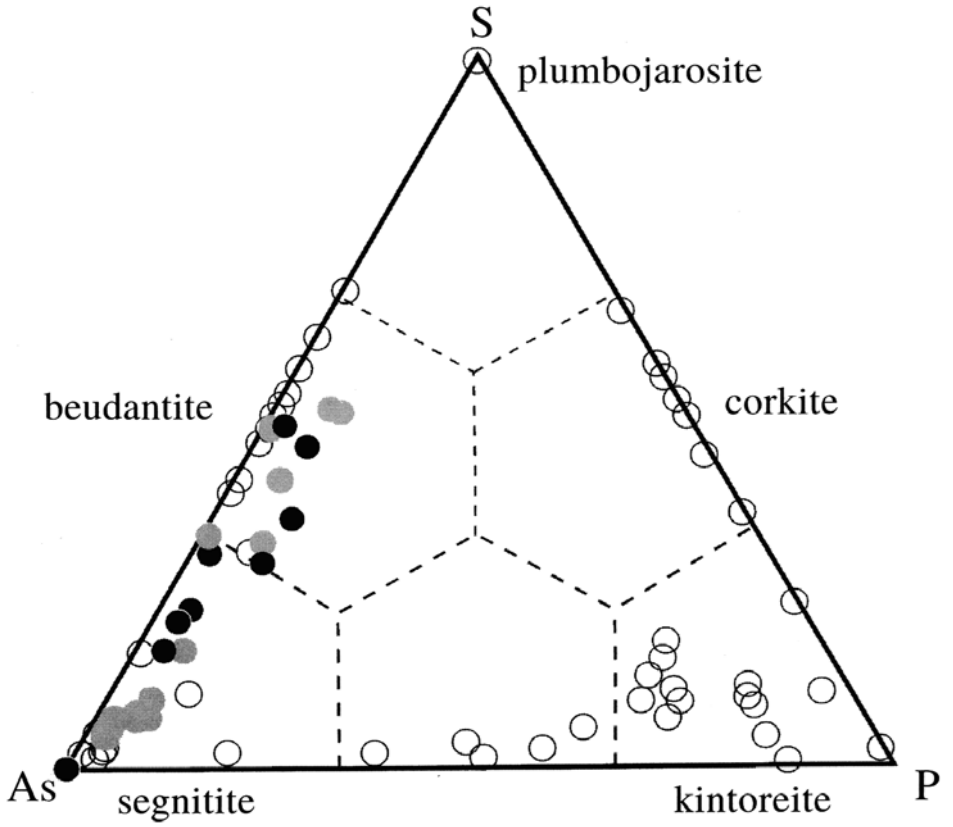

Fig. 13 The As-P-S diagram for Pb and Fe dominant members of the crandallite group. Divided into the fields according to Novák et al. (1994). Black circle – Cínovec samples, gray circle – Moldava samples, open circle – published data.

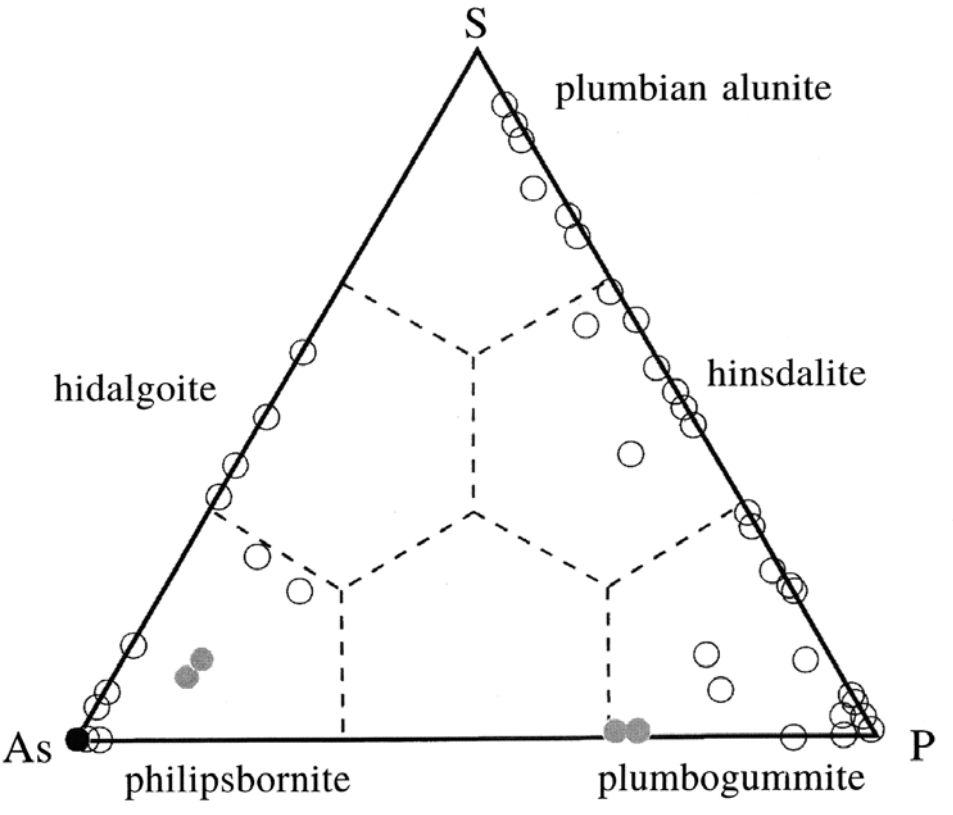

Fig. 14 The As-P-S diagram for Pb and Al dominant members of the crandallite group. Divided into the fields according to Novák et al. (1994). Black circle – Cínovec samples, gray circle – Moldava samples, open circle – published data.

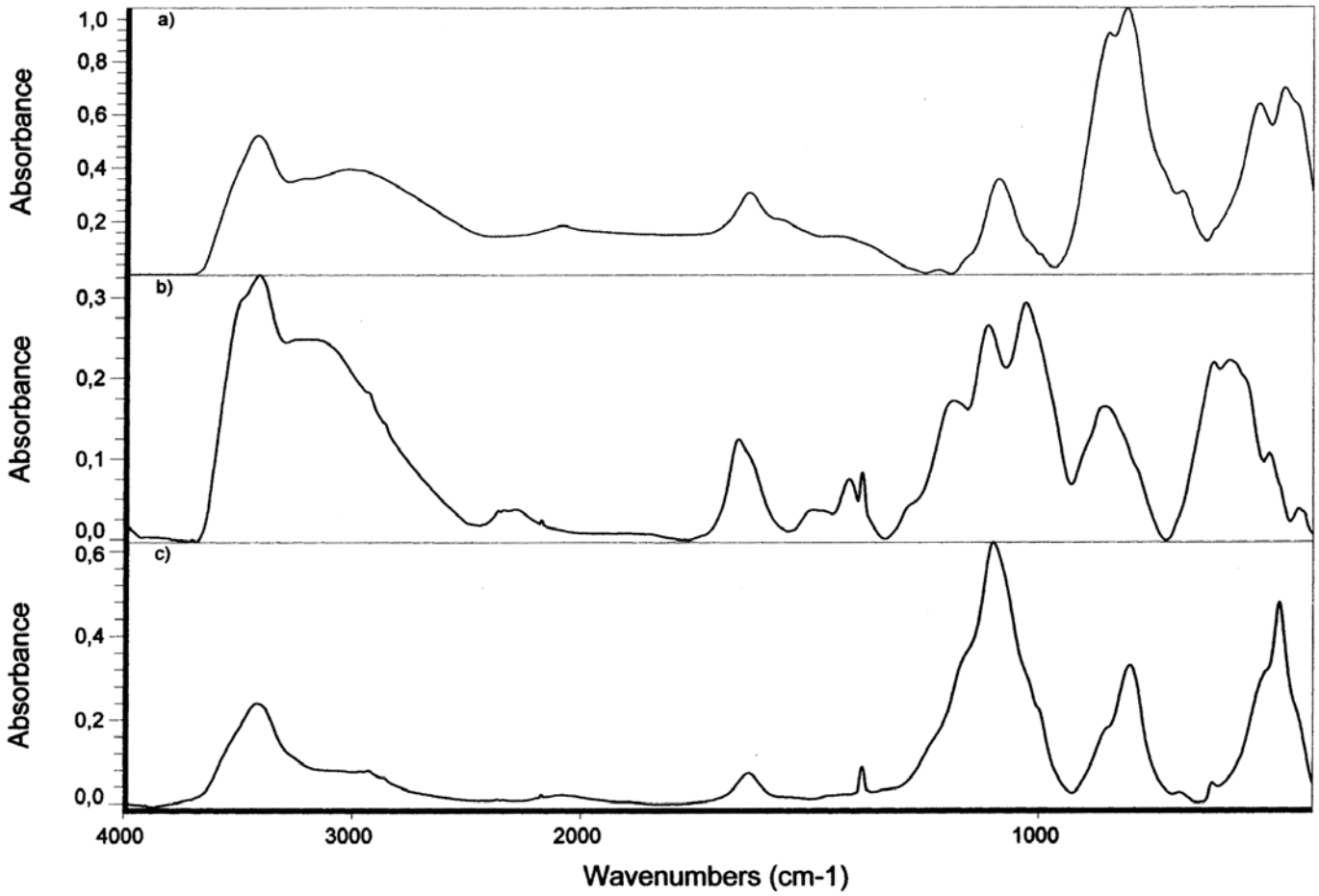

Fig. 15 The infrared absorption spectra of sample studied (KBr disk).
a) segnitite, Moldava; b) plumbogummite, Moldava; c) beudantite, Cínovec

and the δ As-OH out-of-plane bending vibration at 621 cm^{-1} cannot be excluded.

A band at 582 cm^{-1} with a shoulder at 618 cm^{-1} observed in the infrared spectrum of plumbogummite is assigned to the ν_4 PO_4 triply degenerate bending vibrations. A band at 465 cm^{-1} with a shoulder at 509 cm^{-1} (beudantite), at 465 cm^{-1} with a shoulder at 436 cm^{-1} (segnitite) may be connected with the ν_4 AsO_4 triply degenerate bending vibrations, δ AsO_4 bending vibrations, ν_2 SO_4 doubly degenerate bending vibration and probably also O-Fe vibration. A weak band at 430 cm^{-1} with a shoulder at 477 cm^{-1} (plumbogummite) may be assigned to the ν_2 PO_4 doubly degenerate and/or ν_4 AsO_4 triply degenerate and/ /or δ PO_3 or d AsO_3 bending vibrations.

T_d symmetry of phosphate, arsenate and sulfate groups and C_{3v} symmetry of PO_3OH and AsO_3OH groups are lowered. This is characterized by splitting of degenerate vibrations. However, it is difficult to infer the site symmetry of these groups in the structures because of coincidence of related vibrations. It is, therefore, also not unambiguously possible to define the number of these vibrations which may enable to assume structurally non-

Table 7 Infrared absorption spectrum of beudantite from Cínovec.

[cm^{-1}]			Tentative assignment
3573	m	sh	ν OH stretching vibrations
3406	s		
3254	m	sh	
2928	w		
2848	w		
2174	vw		ν OH stretching vibration in AsO_3OH (?)
1634	m		δ H_2O bending vibration
1235	m	sh	ν_3 SO_4 antisymmetric stretching vibration
1169	s	sh	
1100	vs		
1035	s	sh	δ As-OH in-plane vibration
999	m	sh	ν_1 SO_4 symmetric stretching vibration
854	m	sh	ν_3 AsO_4, ν_3 AsO_3 antisymmetric stretching, ν_1 AsO_4 symmetric stretching, δ AsOH out-of-plane bending vibrations
803	s		
687	w		ν_4 SO_4 antisymmetric stretching, δ AsOH bending vibrations
621	w		
509	m	sh	ν_4 AsO_4 bending, ν_2 SO_4 bending, δ AsO_3 bending, O-Fe stretching vibrations
476	s-vs		

FTIR spectrophotometer Nicolet 740, KBr tablet.
Intensity and character of absorption bands: vs – very strong, s – strong, ms – medium strong, m – medium, mw – medium weak, w – weak, vw – very weak; b – broad, sh – shoulder, sr – sharp.

Table 8 Infrared absorption spectrum of plumbogummite from Moldava.

[cm^{-1}]			Tentative assignment
3409	s		ν OH stretching vibrations
3254	m	b	
2362	w		ν OH stretching vibrations in PO_3OH
2301	m		
1656	s	sr	δ H_2O bending vibrations
1619	w	sh	
1496	w	b	δ POH in-plane bending bending vibration or overtones and/or
1414	m	sr	combination bands
1281	m	sh	
1182	s	sh	ν_3 PO_4 antisymmetric stretching vibration
1110	s	sr	ν_3 PO_3 antisymmetric stretching vibration
1029	vs	sr	
851	s	b	ν_3 AsO_4 antisymmetric stretching vibration
784	w	sh	ν_1 AsO_4 symmetric stretching vibration and/or δ POH out-of-plane bending vibration
618	s	sh	ν_4 PO_4 bending vibration
582	s	sr	
477	w	sh	ν_2 PO_4 and/or n_4 AsO_4 and/or δ PO_3 and/or δ AsO_3 bending vibrations
430	w		

FTIR spectrophotometer Nicolet 740, KBr tablet.
Intensity and character of absorption bands: vs – very strong, s – strong, ms – medium strong, m – medium, mw – medium weak, w – weak, vw – very weak; b – broad, sh – shoulder, sr – sharp.

equivalent anion groups present in the structure. This was, therefore, assumed only in the case for plumbogummite (Sejkora et al. 1998).

Nomenclature remarks

The main problem in minerals of the crandallite group is the status of members containing S and P, As in the (XO_4) position. Structural data for many minerals are absent and discrepancies in known data have been found. In the case of ordered arrangement, two independent tetrahedral sites may exist in the structure and the space group R –3m transforms into the nonsymmetric group R 3m. A disorder in the anionic part was observed for svanbergite, beudantite, woodhouseite, kintoreite and hinsdalite (Kato 1971, Kato – Miura, 1977, Szymanski 1988, Giussepetti – Tadini 1989, Kharisun et al. 1997, Kolitsch et al. 1999c). On the contrary, Giussepetti, Tadini (1987) found ordered (PO_4) and (SO_4) arrangements in the structure of corkite, and Jambor et al. (1996) in the case of gallobeudantite. Experimental evidence for the order – disorder in the (XO_4) anion in individual mineral phases of this family, however, is missing. Experimental data and interpretation published for individual minerals, concerning the order – disorder in the tetrahedral site may be often explained in both ways. The small differences found in the R value (e. g. corkite 2.8 % and 3.7 %, kintoreite 3.0. % and 4.7. %) for refinements carried out in the space group R –3m and R 3m can be to a large extent a reflection of Pb atom disorder (e. g. Szymanski 1988). In addition, Radoslavich (1982) found the monoclinic space group Cm for gorceixite and Szymanski (1988) a triclinic cell also in the case of one beudantite crystal.

If atoms P, As and S in tetrahedral sites were disordered, beudantite and svanbergite should be, according to the current IMA nomenclature rules, understood as intermediate members in binary solid solution and not as independent mineral species (Birch et al. 1992). Novák et al. (1994) assume the degree of structure ordering (SO_4)(PO_4) and (AsO_4) groups to be various in the framework of one mineral depending on the genesis of the given phase. The so-called intermediate members are classified according to their status as mineral species on the basis of a possible structure ordering and from the historical point of view.

Conclusions

a) The following members of the Pb-dominant members of crandallite group were unambiguously identified

(1) at the Cínovec deposit: beudantite, segnitite, philipsbornite, and

(2) at the Moldava deposit: beudantite, segnitite, philipsbornite and plumbogummite.

The physicochemical characteristics were given for all the mineral species mentioned.

Table 9 Infrared absorption spectrum of segnitite from Moldava.

[cm^{-1}]			Tentative assignment	
3427	s			
3225	m	sh	ν OH stretching vibrations	
3007	ms	b		
2768	mw	sh		
2094	w		ν OH stretching vibrations in AsO_3OH (?)	
1632	m		δ H_2O bending vibrations	
1554	mw	sh		
1434	m	b		
1277	w			
1214	w		δ As-OH in-plane bending	
1162	w	sh	vibrations	ν_3 SO_4 antisymmetric
1090	s			stretching vibrations
1024	w	sh		
995	w	sh	ν_3 AsO_4, ν_3 AsO_3 antisymmetric stretching,	
849	vs		ν_1 AsO_4 symmetric stretching and δ AsOH out-of-plane	
802	vs		bending vibrations	
748	m	sh	ν AsOH stretching vibrations	
690	m			ν_4 SO_4 antisymmetric
621	w		δ AsOH out-of-plane vibration	stretching vibrations
523	s			
465	s		δ AsO_3 bending vibrations	ν_4 AsO_4 bending vibrations
436	s	sh		

FTIR spectrophotometer Nicolet 740, KBr tablet.
Intensity and character of absorption bands: vs – very strong, s – strong, ms – medium strong, m – medium, mw – medium weak, w – weak, vw – very weak; b – broad, sh – shoulder, sr – sharp.

b) The minority content of indium (up to 2.44 wt. % In_2O_3) in the B position of general formula observed in beudantite sample from Cínovec is the first known assertion of this chemical element in minerals of the crandallite group.

c) The pronounced dependence of the lattice parameters on the Al/Fe ration in B position and As/P in X position of general formula for Pb-dominant members of crandallite group was established. It is interesting that the influence of the sulfate group in the X position on the lattice parameters is considerably low.

d) Extensive isomorphism in all three positions in general formula of the crandallite group minerals was confirmed.

Acknowledgment. We are grateful to RNDr. I. Čejková (National Museum, Prague), RNDr. M. Fengl (Ústí n. L.), M. Radoň (Regional Museum, Teplice), Ing. M. Novotná CSc. (The Institute of Chemical Technology, Prague) and Dr. A. Langrová (Geological Institute, Academy of Science of Czech Republic, Praha) for their kind assistance.

The authors would like to express their thanks to the State Department of Culture which has supported this research with its projects RK99P03OMG008 and VZF02/98:NMPM00001.

Submitted May 10, 2000

References

Birch, W. D. – Pring, A. – Gatehouse, B. M. (1992): Segnitite, $PbFe_3H(AsO_4)_2(OH)_6$, a new mineral in the lusungite group from Broken Hill, New South Wales, Australia. – Am. Mineral., 77: 656–659.

Bischoff, W. (1999): Segnitit von St. Andreasberg im Harz. – Aufschluss, 50: 102–104.

Blount, A. M. (1974): The crystal structure of crandallite. – Am. Mineral., 59: 41–47.

Burnham, Ch. W. (1962): Lattice constants refinement. – Carnegie Inst. Washington Year-book, 61: 132–135.

Brophy, G. P. – Scott, E. S. – Snellgrove, R. A. (1962): Sulfate studies 2. Solid solution between alunite and jarosite. – Am. Mineral., 47: 112–126

David, J. – Jansa, J. – Novák, F. – Prachař, I. (1990): Philipsbornite from the Sn-W deposit Cínovec in the Krušné hory Mts. (Czechoslovakia). – Věst. Ústř. Úst. geol., 65: 367–369.

Farmer, V. C. (Ed.) (1974): The infrared spectra of minerals. – Mineral. Soc. Monograph., 4, 539 pp.

Fengl, M. – Jansa, J. – Novák, F. – Reichmann, F. (1981): Mineralogy of the supergene zone of fluorite deposit Moldava in Krušné hory Mts. – Sbor. geol. Věd., R. TG 17 (in Czech).

Gevorkyan, S. V. – Petrunina, A. A. – Povarennykh, A. S. (1976): IR-spectroscopic and X-ray studies of crandallite group minerals. – Constitution and properties of minerals, 10: 54–59 (in Russian).

Giusepetti, G. – Tadini, C. (1987): Corkite, $PbFe_3(SO_4)(PO_4)(OH)_6$, its crystal structure and order arrangement of the tetrahedral cations. – N. Jb. Miner. Mh., 19: 71–81.

– (1989): Beudantite $PbFe_3(SO_4)(AsO_4)(OH)_6$, its crystal structure, tetrahedral site disordering and scattered Pb distribution. – N. Jb. Miner., Mh. 27–33.

Hendricks, S. B. (1937): The crystal structure of alunite and jarosite. – Am. Mineral., 22: 273.

Jambor, J. L. – Dutrizac, J. E. (1983): Beaverite – plumbojarosite solid solutions. – Can. Mineral., 21: 101–113.

Jambor, J. L. – Owens, D. R. – Grice, J. D. – Feinglos, M. N. (1996): Gallobeudantite, $PbGa_3[(AsO_4), (SO_4)]_2(OH)_6$, a new mineral species from Tsumeb, Namibia, and associated new gallium analogues of the alunite – jarosite family. – Can. Mineral., 34: 1305–1315.

Jansa, J. – Novák, F. – Pauliš, P. – Scharmová, M. (1998): Supergenní minerály Sn-W ložiska Cínovec v Krušných horách (Česká republika). – Bull. mineral.-petrolog. Odd. Nár. Muz. (Praha), 6: 83–101. (in Czech)

Kato, T. (1971): The crystal structure of goyazite and woodhouseite. – N. Jb. Miner. Mh., 241–247.

– (1977): Further refinement of the woodhouseite structure. – N. Jb. Miner. Mh., 54–58.

Kato, T. – Miura, Y. (1977): The crystal structure of jarosite and svanbergite. – Min. Jour., 8(8): 419–430.

Keller, P. (1971): Die Kristallchemie der Phosphat- und Arsenat Minerale unter besonder Berücksichtigung der Kationen-Koordinationspolyeder und des Kristallwassers. Teil I: Die Anionen der Phosphat- und Arsenatminerale. – N. Jb. Miner. Mh., 491–510.

Kharisun – Taylor, M. R. – Bevan, D. J. M. (1997): The crystal structure of kintoreite, $PbFe_3(PO_4)_2(OH, H_2O)_6$. – Mineral. Mag., 61: 123–129.

Kolitsch, U. – Slade, P. G. – Tiekink, E. R. T. – Pring, A. (1999a): The structure of antimonian dussertite and the role of antimony in oxysalt minerals. – Min. Mag., 63(1): 17–26.

Kolitsch, U. – Taylor, M. R. – Fallon, G. D. – Pring, A. (1999b): Springcreekite, $Ba\ V^{3+}_3(PO_4)_2(OH, H_2O)_6$, a new member of the crandallite group, from the Spring Creek mine, South Australia: first natural V^{3+} member of the alunite family and its crystal structure. – N. Jb. Miner. Mh., 12: 529–544.

Kolitsch, U. – Tiekink, E. R. T. – Slade, P. G. – Taylor, M. R. – Pring, A. (1999c): Hinsdalite and plumbogummite, their atomic arrangements and disordered lead sites. – Eur. J. Mineral., 11: 513–520.

Lengeauer, C. L. – Giester, G. – Irran, E. (1994): $KCr_3(SO_4)_2(OH)_6$: Synthesis, characterization, powder diffraction data and structure refinement by the Rietveld technique and a compilation of alunite-type compounds. – Powder Diffract., 9(4): 265–271.

Liferovich, R. P. – Yakovenchuk, V. N. – Pakhomovsky, Ya. A. – Bogdanova, A. N. – Stümpel, G. (1999): Crandallite, goyazite and gorceixite from the Kovdor massif, Russia. – N. Jb. Miner. Mh., 4: 145–166.

Mandarino, J. A. (1999): Fleischer's Glossary of Mineral Species. – 8th Ed., Mineralogical Record, Tucson, 225 pp.

Myneni, S. C. B. – Traina, S. J. – Waychunas, G. A. – Logan, T. J. (1998): Experimental and theoretical vibrational spectroscopic evaluation of arsenate coordination in aqueous solutions, solids, and at mineral – water interfaces. – Geochim. Cosmochim. Acta, 62: 3285–3300.

Novák, F. – Jansa, J. – Pauliš, P. (1995): Die Indium Mineralization der Sn-W lagerstätte Zinwald (Cínovec) im Erzgebirge (Krušné hory), Tschechien. – Mineralien Welt, 6(1): 47–48.

Novák, F. – Jansa, J. – Prachař, I. (1994): Classification and nomenclature of alunite – jarosite and related mineral groups. – Věst. Čes. geol. úst., 69(2): 51–57.

Ondruš, P. (1995): ZDS – software for analysis of X-ray powder diffraction patterns. Version 6.01. User´s guide. – Prague, 208 pp.

Pabst, A. (1947): Some computations on svanbergite, woodhouseite and alunite. – Am. Mineral., 32: 16.

Pring, A. – Birch, W. D. – Dawe, J. – Taylor, M. – Deliens, M. – Walenta, K. (1995): Kintoreite, $PbFe_3(PO_4)_2(OH, H_2O)_6$, a new mineral of the jarosite-alunite family, and lusungite discredited. – Mineral. Mag., 59: 143–148.

Radoslavich, E. W. (1982): Refinement of gorceixite structure in Cm. – N. Jb. Miner. Mh., 446–464.

Rattray, K. J. – Taylor, M. R. – Bevan, D. J. M. – Pring, A. (1996): Compositional segregation and solid solution in the lead dominant alunite-type minerals from Broken Hill, N. S. W. – Mineral. Mag., 60: 779–785.

Sasaki, K. – Tanaike, O. – Konno, H. (1998): Distinction of jarosite-group compounds by Raman spectroscopy. – Can. Mineral., 36: 1225–1235.

Scharm, B. – Scharmová, M. (1995): Minerals of crandallite group. – Bull. mineral.-petrolog. Odd. Nár. Muz. (Praha), 3: 172–177. (in Czech)

Schmetzer, K. – Tremmel, G. – Medenbach, O. (1982): Philipsbornite $PbAl_3H[(OH)_6(AsO_4)_2]$ from Tsumeb, Namibia – a second occurrence. – N. Jb. Miner. Mh., 248–254.

Scott, K. M. (1987): Solid solution in, and classification of gossan-derived members of the alunite-jarosite family, northwest Queens-land, Australia. – Am. Mineral., 72: 178–187.

Sejkora, J. – Čejka, J. – Šrein, V. – Novotná, M. – Ederová, J. (1998): Minerals of the plumbogummite-philipsbornite series from Moldava deposit, Krušné hory Mts., Czech Republic. – N. Jb. Miner. Mh., 4: 145–163.

Sejkora, J. – Řídkošil, T. (1994): Tetrarooseveltite, β-$BiAsO_4$, a new mineral species from Moldava deposit, the Krušné hory Mts., Northwestern Bohemia, Czech Republic. – N. Jb. Miner. Mh., 4: 179–184.

Sejkora, J. – Řídkošil, T. – Šrein. V. (1994): Rooseveltite from Moldava, Krušné hory, Mts., Czech Republic. – N. Jb. Miner. Mh., 1: 40–48.

Somina, M. J. – Bulach, A. G. (1966): Florencite from the Eastern Sajany carbonatites and some question of chemistry of the crandallite group minerals. – Zap. Vsesoyuz. Min. Obsch. 95: 537–550. (in Russian)

Szymanski, J. T. (1988): The crystal structure of beudantite, $Pb(Fe, Al)_3[(As, S)O_4]_2(OH)_6$. – Can. Mineral., 26: 923–933.

Walenta, K. – Zwiener, M. – Dunn, P. J. (1982): Philipsbornite, a new mineral of the crandallite series from Dundas, Tasmania. – N. Jb. Miner. Mh., 1–5.

Yvon, K. – Jeitschko, W. – Parthe, E. (1977): LAZY PULVERIX – a computer program for calculating theoretical X-ray and neutron diffraction powder patterns. – J. Appl. Cryst., 10: 73–74.

Pb dominantní členy skupiny crandallitu z ložisek Cínovec a Moldava, Krušné hory (Česká republika)

Pb dominantní členy skupiny crandallitu z Sn-W ložiska Cínovec a fluoritového ložiska Moldava (Krušné hory, Česká republika) byly studovány pomocí rentgenové práškové difrakce, chemických analýz a infračervené spektroskopie. Ve vzorku beudantitu z Cínovce byl zjistěn minoritní obsah india (do 2.44 hmot. % In_2O_3) v B pozici obecného vzorce, který je prvním známým uplatněním tohoto chemického prvku v minerálech skupiny crandallitu. Zjištěna byla významná závislost hodnot mřížkových parametrů jednotlivých Pb dominantních členů skupiny crandallitu na poměru Al/Fe v B pozici a As/P v X pozici obecného vzorce. Nově byla i potvrzena rozsáhlá izomorfie ve všech třech pozicích obecného vzorce minerálů této skupiny.